Photochemical Reaction of Diazomethane with Hydrogen-Terminated Silicon Surfaces

Lars H. Lie, Samson N. Patole, Edward R. Hart, Andrew Houlton,* and Benjamin R. Horrocks*

Department of Chemistry, Bedson Building, University of Newcastle upon Tyne, Newcastle upon Tyne, NE1 7RU, U.K.

Received: August 14, 2001; In Final Form: October 19, 2001

Diazomethane reacts with hydrogen-terminated porous or single crystal silicon surfaces under irradiation with the 365 nm line from a mercury lamp. The surface Si−H_x groups are lost and an HF-resistant, polymeric hydrocarbon species is formed. The mechanism is proposed to commence with insertion of singlet methylene into the Si−H bond as in the analogous reaction of molecular hydrosilanes. However, the infrared spectra indicate that $-CH_2-$ groups rather than terminal $-CH_3$ are dominant on the surface after reaction. This is attributed to an oligomerization which may proceed via attack of singlet methylene on C−H bonds or via a radical process. In the case of porous silicon, significant oxidation occurs in parallel to the reaction with diazomethane due to the presence of trace water from the reagents used to generate diazomethane. The oxidized silicon species can, however, be removed selectively by washing in aqueous 48% HF without affecting the integrated intensity of the C−H stretching bands observed by FTIR spectroscopy. In combination with an analysis of the IR spectroscopic data, we conclude that the hydrocarbon species on the surface are anchored via robust Si−C bonds rather than the labile Si−O−C linkage. This is further supported by the stability of diazomethane-treated, polished single crystal wafers to in-air STM and electrochemical cycling in aqueous media. The diazomethane treatment also shifts the flatband potential in a negative direction in aqueous NaCl compared to Si(111)−H surfaces.

Introduction

The surface chemistry of silicon is of increasing interest in semiconductor science and technology. Silicon-bound organic monolayers are important in both fundamental studies (for reviews of the area see refs 1−3) and applications arising from the technological importance of silicon in microelectronics, sensors, and photovoltaics.[4−12] Examples include immobilization of DNA,[13] electronic passivation,[14] incorporation of biochemical functionality at interfaces,[15] and polymers.[16,17] In addition, methods for chemical modification of porous silicon surfaces can be used to manipulate its photoluminescence, spectroscopic, and electrochemiluminescent behavior.[1,2,18−20] Organic monolayers can be formed at single crystal and porous silicon surfaces via oxidation followed by treatment with trichlorosilane reagents[21] or by using chemistry analogous to that of molecular hydrosilanes to modify the hydrogen-terminated surface produced by fluoride etchants.[1−3] Well-ordered monolayers may be formed on single crystal silicon surfaces by either route. However, for some electrochemical applications, an intervening oxide layer is undesirable and monolayers which are directly bonded to the silicon introduce less electrical resistance. A rich chemistry of the hydrogen-terminated surface is now known and either Si−O−C,[23−28] Si−N,[29] or Si−C[3,22,30−32] bonded monolayers can be prepared. Si−C bonded monolayers are more robust toward atmospheric oxidation and attack by aqueous solutions than, e.g., Si−O−C bonded monolayers.[3,25,27] Monolayers anchored to the surface by an Si−C bond may be prepared by reaction of unsaturated molecules using heat,[30,33] light,[34,35] electrochemistry,[36] hydrosilation catalysts,[18,37] or radical initiators.[22] Methoxy and methyl monolayers, which may be expected to introduce the least electrical resistance, can be synthesized by reactions of methanol,[23,38,39] Grignard reagents,[5,40] by electrochemical reduction of methyl halides, or anodization in the presence of Grignard reagents.[41−43]

We report here the reaction of singlet methylene with H-terminated single crystal or porous silicon surfaces by photolysis in the presence of diazomethane. The insertion of singlet methylene into Si−H bonds is known from molecular hydrosilane chemistry; however, it has not been reported previously on the hydrogen-terminated silicon surface and appears to be fundamentally different from known reactions of this surface that involve nucleophilic attack,[24,44] hydride transfer,[45] radical mechanisms,[22,33,34,41−43,46] or catalytic hydrosilation.[18,19,37] Molecular hydrosilanes react with diazomethane under illumination according to eq 1:

$$R_3Si-H \xrightarrow[\lambda = 365\ nm]{CH_2N_2,\ h\nu} R_3Si-CH_3 \rightarrow R_3Si-CH_2CH_3 \rightarrow \quad (1)$$

The first excited state of diazomethane is only weakly bound and the reactive species is thought to be singlet methylene, which inserts directly into the Si−H bond.[47−49] The rate of insertion into Si−H bonds in methylsilane is ca. 9 times faster than the insertion into the C−H bonds.[49] An alternative mechanism in which the less reactive triplet ground state of methylene abstracts a hydrogen atom and the methyl and silyl radicals formed recombine after one of the electron spins is flipped is thought to be a minor process (∼20%), at least in the gas phase.[50] Evidence for the direct insertion of singlet methylene into C−H bonds comes from studies of the product distribution and influence of radical traps on the reaction between *n*-alkanes and diazomethane under photolytic conditions. Reaction with C−H bonds often proceeds with retention of configuration,[50] which

* Corresponding authors: b.r.horrocks@ncl.ac.uk; andrew.houlton@ncl.ac.uk

10.1021/jp013148t CCC: $22.00
Published on Web 12/12/2001

indicates direct insertion. However, both retention of configuration and racemization are observed with compounds containing the more reactive Si−H bond;[51] this indicates a role for the triplet carbene and a radical mechanism. Further reaction between methylene and C−H bonds, or with diazomethane itself, to form higher alkanes and also alkenes is known.[52]

Experimental Section

Single Crystal and Abraded Silicon. ⟨111⟩ or ⟨100⟩ oriented silicon wafers (boron-doped, p-type, 10 Ω cm resistivity, Compart Technology, Peterborough, U.K.) were degreased in acetone before production of a clean oxide layer by immersion in freshly prepared piranha solution (1:1 v/v concentrated H_2SO_4 and 30% H_2O_2) for 10 min at room temperature. The oxide was removed and a hydride layer formed by a subsequent immersion in 48% w/w aqueous HF (10 min). Wafers were then rinsed for 20 s in deionized water (Millipore, 18 MΩ cm) and blown dry with N_2. Abraded silicon wafers were prepared as described previously.[39] Briefly, mechanical abrasion of both faces of the silicon wafer followed by repeated oxidation in piranha solution and etching with aqueous HF increases the surface area and the signal-to-noise ratio in transmission FTIR spectroscopy. Facets of ⟨111⟩ orientation are also produced and the majority of the Si−H vibrations are characteristic of this surface with some additional features in the Si−H stretching region due to the presence of atomic-scale disorder.[39]

Porous Silicon. Porous silicon was formed by galvanostatic anodization of boron-doped p-Si⟨100⟩ oriented wafer (10 Ω cm resistivity, Compart Technology, Peterborough, U.K.). The electrolyte was a 1:1 v/v solution of 48% aqueous HF and ethanol in a Teflon cell, and a current density of 1−100 mA cm^{-2} was applied until the charge passed reached 4.9 C cm^{-2}. The porous silicon was then washed in deionized water (Millipore, 18 MΩ cm) to remove ethanol, rinsed with hexane, and dried in a stream of dry N_2. Any residual water in the pores was removed by heating to ca. 100 °C overnight on a standard vacuum line possessing entirely grease-free joints such as Young's taps. The porous silicon samples were then stored at room temperature, also under vacuum. Transmission FTIR spectra indicated that samples so prepared could be stored under vacuum for several days and were hydrogen-terminated with no oxide present and no hydrocarbon contamination.

Preparation of Diazomethane. Diazomethane was prepared by a conventional route in which *N*-methyl-*N*-nitrosotoluene-*p*-sulfonamide in ether is treated with KOH/ethanol and distilled with a stream of dry nitrogen passing through the solution. The vapor was collected in an ice-cooled, flat-bottomed receiving flask containing dry ether to yield a solution of diazomethane in ether.[53] To minimize the risk of detonation, samples of porous, single crystal or abraded silicon wafers were placed "face-down" directly in the glass receiving flask under ether before collection of the diazomethane. The samples were then illuminated through the base of the flask at $\lambda = 365$ nm for 2 h using a mercury-based pen lamp (Mineralight, San Gabriel, CA) placed underneath the flask.

Infrared Spectroscopy, Optical Microscopy and Scanning Tunneling Microscopy. Interference from atmospheric CO_2 and H_2O in the infrared spectra was minimized by flushing the spectrometer optics and sample compartment with dry nitrogen. Spectra (unpolarized) were obtained using a Biorad FTS-40 spectrometer fitted with a deuterated triglycine sulfate (DTGS) detector in the normal transmission alignment. Some optical microphotographs of porous silicon were taken using a conventional optical microscope (Leitz Laborlux 12 ME S) and saved as bitmap files using a frame grabber (DT3155, Data Translation, Marlboro, MA) and CCD camera (PULNiX, model TM-6EX, Basingstoke, U.K.).

STM images of hydrogen-terminated and diazomethane-treated silicon surfaces in air were obtained using a Nanosurf Easyscan instrument (Nanosurf AG, Basel, Switzerland). The STM was modified in-house by construction of a small glass chamber and a new steel vibration-isolation platform. The glass chamber was sealed to the steel via an O-ring and three screw-clamps. This modification enabled us to control the atmosphere during imaging by flushing with air, nitrogen or evacuating the chamber with a rotary pump (Leybold Ltd, London, U.K., "Mini" pump, low vacuum only). Tips were prepared by electrochemical etching of 80/20 Pt/Ir alloy wire in 1 M HCl/saturated $CaCl_2$ using ca. 20 V a.c. Silicon wafers, oriented ⟨111⟩ for STM, were obtained from the same sources as for the infrared and electrochemical studies (Compart Technology, Peterborough, U.K.). The wafers were phosphorus-doped *n*-type and had a resistivity in the range 1−20 Ω cm. Ohmic contact to the back of the wafer was made by rubbing In/Ga eutectic onto the wafer.

Electrochemistry. Cyclic voltammetry (CV) and impedance spectroscopy (EIS) were carried out in a PTFE cell with the silicon electrode sealed to the base via an O-ring. The wetted area of the silicon was 0.283 cm^2. Ohmic contact to the silicon electrodes was made as for the STM experiments. For both impedance spectroscopy and cyclic voltammetry an Ag/AgCl reference electrode was used and the electrolyte was either 0.1 M NaCl or KCl. The auxiliary electrode was a Pt wire for cyclic voltammetry; however, for the impedance measurements the background d.c. currents were sufficiently low (<1 μA cm^{-2}) to employ a two-electrode cell with a dual auxiliary/reference Ag/AgCl electrode. The silicon electrode was illuminated with unfocused white light from a 100 W tungsten lamp during cyclic voltammetry. Although a quantitative study of the photocurrent was not made, the level of illumination was more than sufficient to obtain diffusion-controlled peak currents in CV for both oxidation and reduction at the low concentration of redox species (1 mM $Ru(NH_3)_6Cl_3$) used. No redox couple was added for the impedance measurements and the electrode was not illuminated. The potentiostat for CV was an EG&G model 263A (EG&G PAR, Princeton, NJ) and the impedance spectra were obtained using an 1187 Solartron electrochemical interface and a 1253 gain-phase analyzer (Solartron, Farnborough, U.K.) using software written in-house. Impedance spectra were collected over the range 200−5000 Hz at each d.c. potential reported, and the capacitance was determined by fitting the data to an equivalent circuit consisting of the double layer capacitance in series with the cell resistance. All the data presented were consistent with such a model; the Nyquist diagram showed a line approximately normal (ca. 80 degrees) to the real axis. Impedance spectra at extreme potentials were found to deviate from the simple model and to display features characteristic of significant faradaic reaction. Such data were not analyzed due to the comparatively large uncertainties in the computed capacitances.

Calculations. Assignment of the IR spectra and interpretation of the impedance spectra were aided by ab initio and density functional calculations on small molecule models of the silicon surface. We have previously found that small silicon clusters [e.g., $(H_3Si)_3Si-H$] provide reasonable models of the localized vibrational modes.[54] Density functional calculations were carried out using the Titan program package[55] and ab initio calculations using the PC GAMESS version[56] of the GAMESS (US)

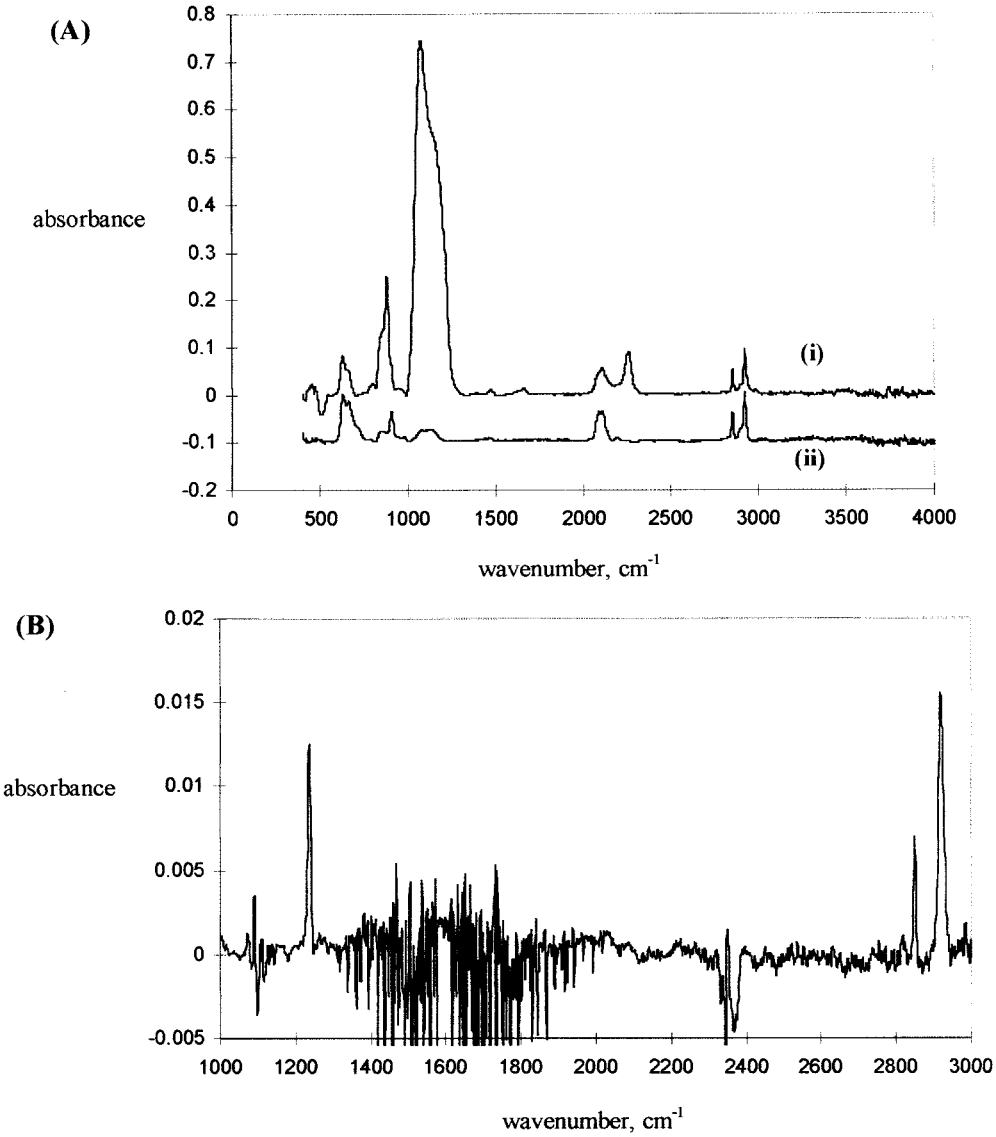

Figure 1. (A) Infrared spectra of porous silicon after photolysis in diazomethane/ether for 2 h. The resolution was 2 cm^{-1} and 100 scans were coadded and averaged. (i) diazomethane/$h\nu$-treated porous silicon, (ii) diazomethane/$h\nu$-treated porous silicon after washing with 48% aqueous HF. (B) Infrared spectra of abraded silicon after photolysis in diazomethane/ether for 2 h. The resolution was 1 cm^{-1} and 1000 scans were coadded and averaged.

quantum chemistry package.[57] Finite field calculations using GAMESS employed the higher precision Rys polynomial integral code and tighter cutoffs suggested in the GAMESS reference documentation.[57]

Results and Discussion

Porous Silicon. When porous silicon was allowed to stand in ethereal diazomethane in the absence of irradiation, only small amounts of C−H stretching vibrations and growth of oxide-related bands at 2250 and ∼1100 cm^{-1} in the IR spectrum were observed. Increased C−H stretching intensity was observed after illumination. Since we carried out the reaction in glass apparatus with illumination of the porous silicon from an external mercury lamp, wavelengths below approximately 300 nm were absorbed by the glass walls of the reaction flask. UV-vis spectra of samples of this glass confirmed that the majority of the useful light corresponded to the 365 nm mercury line. After photolysis in the solution of CH_2N_2, the IR absorption spectrum (Figure 1A, Table 1) of porous silicon shows several new bands due to C−H vibrations at 2918, 2850, and 1471 cm^{-1}, which we interpret as due to the formation of a surface Si−C bonded species. The first two bands are the asymmetric and symmetric C−H stretching vibrations. The higher frequency band is more intense; this is consistent with the IR spectrum of a film of polythene and also for isolated methyl groups. However, the frequency of 2918 cm^{-1} is too low for a silicon-bound methyl group[41−43] (expected at ca. 2960 cm^{-1}). There is no sign of the

TABLE 1: Experimental Infrared Spectral Data for Abraded and Porous Silicon after Photolysis in Diazomethane/Ether[a]

vibration	abraded Si [⟨111⟩ facets]	porous silicon/ CH_2N_2	polythene film
CH str ν_{asym}	2918 (17)	2918 (19)	2922 (∼50)
CH str ν_{sym}	2850 (7)	2850 (14)	2846
Si−H str		2104	
O_xSi−H str		2252	
CH_x def.	obscured[b]	1471	1463
Si−CH_x def.	1238		

[a] Note: The table entries are wavenumbers, cm^{-1} and peak widths at half-height are given in parentheses for the C−H stretching vibrations where available. [b] Obscured by features due to water miscancellation due to the low absorbances at abraded compared to porous silicon.

2960 cm^{-1} shoulder that appears in spectra of *n*-alkyl monolayers[58] on porous silicon and the C−H region of the spectrum is closer to that of polythene (Table 1). The asymmetric C−H stretching band in the polythene spectrum is broader and individual contributions to the C−H stretching bands were resolved; however, this spectrum was acquired with a film of high molecular weight polymer, whereas the species on the silicon surface are likely to comprise lower molecular weight fragments. The large Si−O band centered around 1100 cm^{-1} indicates that substantial oxidation of the surface has also occurred, and this is confirmed by the band at 2250 cm^{-1}, which is known to be due to Si−H stretches where the Si atom is back-bonded to O atoms.[59−61] We were not able to avoid such oxidation on porous silicon; however, no significant oxidation of the abraded surface was observed (Figure 1B). This is a consequence of the high sensitivity of porous silicon to wet organic solvents[62] and the trace water that is inevitably present because the preparation of diazomethane involves a KOH/ethanol/H_2O reagent.

Since methylene is known to react rapidly with alcohols to form methoxy ethers, we considered the possibility that the surface termination is actually Si−OCH_3; however, this is inconsistent with the spectra of methoxylated porous and abrade silicon, in which the −CH_3 asymmetric stretches are not degenerate and for which the observed frequencies are slightly higher (ca. 2947 cm^{-1}).[39] The formation of an Si−C rather than an Si−O−C bond is further supported by the absence of any change in the C−H stretch integrated intensity after washing with 48% aqueous HF, which selectively removed most of the oxygen-related bands. The band at ca. 1660 cm^{-1}, characteristic of C═C stretching vibrations, is not expected for a purely alkyl-terminated silicon surface. However, it is known that photolysis of diazomethane produces significant quantities of alkenes and also ethyne due to complex series of reactions of methylene with diazomethane itself.[52] We do not assign this band to unsaturated molecules bound to the silicon surface for several reasons: (i) the C═C stretching mode has also been reported to shift to lower wavenumbers by 40 cm^{-1} or more when one of the vinylic carbons is bonded to the silicon surface,[19] (ii) the peak we observed was removed on washing the porous silicon with HF after the diazomethane treatment, which indicates that the species responsible is not bound through a covalent Si−C bond, and (iii) the 1660 cm^{-1} feature is not associated with the species responsible for the majority of C−H bonds on the surface since these are not affected by the HF washing procedures. We did not observe this peak on the abraded silicon samples (vide infra) and therefore suggest that it is due to alkenes physically trapped within the porous structure; however, insufficient data are available to definitively rule out physisorbed species containing C═O bonds formed by reaction of methylene with trace oxygen.[52]

Effect of Porous Silicon Growth Conditions: Current Density. The current density employed in the anodic etching process to form porous silicon is well known to affect the structure of the porous layer and also the color.[63,64] At low current densities (1−20 mA cm^{-2}) a dark, almost black, film was observed, but at higher current densities (ca. 100 mA cm^{-2}) the film appears yellow and there is a range of darker or lighter green colors at intermediate current densities. We also observe trends in the mechanical stability and chemical reactivity of the porous layer, with those layers formed at high current density being most susceptible to cracking and oxidation under ambient conditions, whereas the low current density films retain a mirror-like surface finish to the eye after drying. Optical micrographs of the low current density material at up to ×500 magnification show an almost featureless surface, whereas the high current density material usually has a large number of fine cracks and visible roughness when viewed at ×500 magnification (Supporting Information 1).

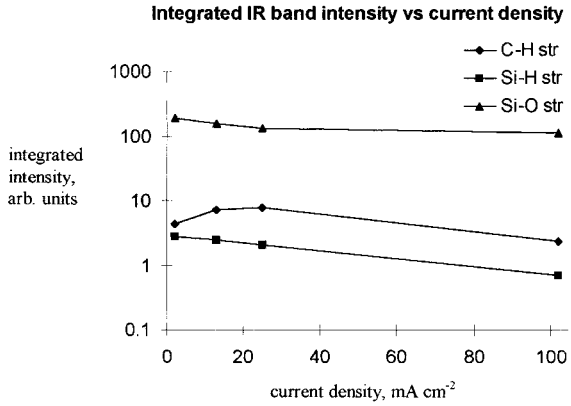

Figure 2. Integrated band intensity (Si−H stretch, Si−O stretch and CH_2 asymmetric + CH_2 symmetric stretches) for diazomethane/*hν*-treated porous silicon versus current density used to prepare the porous silicon.

These differences suggested that a careful choice of current density could be used to control the extent of oxidation in the diazomethane reaction. Indeed, we observed that the current density used to form the porous layer affected the amount of reaction as judged by the integrated intensities of the C−H and Si−O stretches (Figure 2). The C−H stretching intensity increased with decreasing current density, then reached a maximum and fell to small values at the lowest current densities investigated. The optimum value for incorporation of C−H species was at around 40 mA cm^{-2}, whereas the extent of oxidation decreased monotonically with current density (Figure 2). These results can be rationalized by considering that the specific surface area of the porous layer is greatest at low current density, as judged by the integrated Si−H intensity, but that the ethereal diazomethane solution either cannot penetrate the microporosity or the original etch solution is trapped therein. The high current density material is likely to be more accessible to solution-phase reagents due to the presence of microscopic cracks and larger pores. The competition between surface area and accessibility can then result in a maximum for the intensity of the hydrocarbon bands at ca. 40 mA cm^{-2}.

Abraded Silicon. The reaction of diazomethane with abraded silicon was also studied since this material has a reactivity similar to Si⟨111⟩ wafers but allows simple normal transmission IR spectroscopic analysis over the full mid-IR range in contrast to standard internal reflection techniques. Figure 1B shows the absorption spectrum of an abraded Si⟨100⟩ wafer after reaction with diazomethane and referenced to a background consisting of an abraded sample that was not HF-etched. No Si−H stretches are visible, indicating that most of the Si−H bonds have reacted. Steric considerations make it unlikely that all the Si−H bonds are replaced with Si−C bonds.[68] Instead, the formation of Si−OH groups, as originally proposed during the formation of Si−C bonded monolayers from alkenes,[22b] may occur. It is possible that some unreacted Si−H is present since this band has previously been suggested to undergo very considerable heterogeneous broadening upon monolayer formation.[65] The extent of oxidation at abraded silicon after diazomethane photolysis is greatly reduced compared to that at porous silicon, and no O_xSi−H stretching bands are visible at 2250 cm^{-1}. The usual broad Si−O stretching band at 1100 cm^{-1},

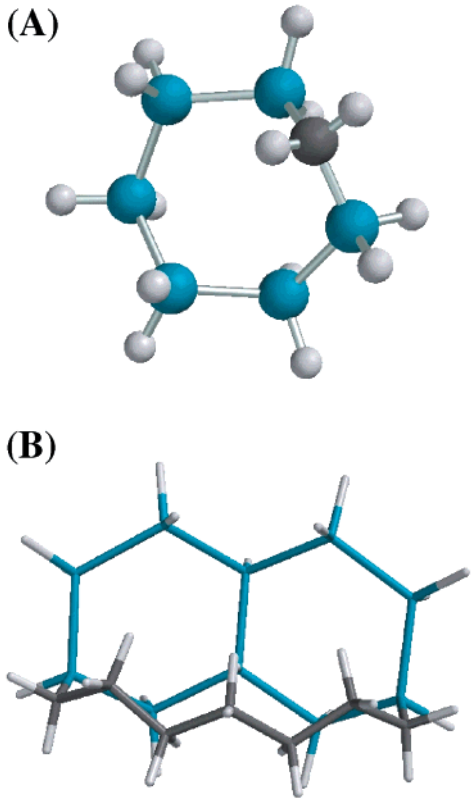

Figure 3. Molecular models of CH_2-containing surface species. Geometries were optimized by DFT calculations at the B3LYP/6-31G(d) level. Si−Si bonds in blue, C−C bonds in black.

which is indicative of oxidation, was also not detectable above the noise level in this region of the spectrum. The abraded silicon surface is generally less reactive and less susceptible to oxidation than porous silicon. Sharp alkyl C−H stretching vibrations were observed at 2918 and 2850 cm^{-1}. The expected CH deformation band at 1471 cm^{-1} is obscured by features due to water miscancellation; however, a $Si-CH_2R$ deformation vibration at 1238 cm^{-1} is clearly visible because of the absence of Si−O stretching vibrations. Such a band is typically observed in ethyl-substituted silicon compounds and also in longer alkyl chains attached to silicon, but with decreased intensity.[73] This band is weak and obscured by residual oxide bands in the HF-etched samples of porous silicon which may indicate that the product of the reaction at porous silicon contains longer hydrocarbon chains than that on abraded silicon. It is also worth noting that, compared to the corresponding data for porous silicon in Table 1, the band at 2850 cm^{-1} in the abraded silicon is quite sharp with a peak width at half-height of 7 cm^{-1}. This suggests that there is a dominant single type of CH_2 species on the surface. In some samples we also observed a band at ca. 900 cm^{-1}, which has been reported previously by us on abraded silicon samples treated with methanol. This vibration is not expected for a purely alkyl terminated surface; we tentatively interpret the band as originating from silanol sites.[39]

Several types of surface species are, in principle, consistent with the infrared spectra: (a) insertion of CH_2 into Si−Si bonds and (b) polymerization of methylene groups covalently attached via Si−C bonds (Figure 3). The insertion of CH_2 into Si−Si bonds would explain the absence of methyl stretching vibrations in the infrared spectra; however, it does not explain the loss of Si−H species observed, and, further, the insertion of CH_2 requires significant distortion of the surface structure. Polymeric species of the general form shown in Figure 3b are consistent with all the spectroscopic observations, but we cannot exclude the possibility of some additional short chain alkyl groups whose concentration is too small for the methyl C−H stretching band at 2960 cm^{-1} to be detectable.

Cyclic Voltammetry And Surface Topography of N−Si Electrodes. Cyclic voltammetry of polished p-type single-crystal wafers of ⟨111⟩ and ⟨100⟩ orientations under illumination with a 100 W tungsten lamp was carried out to determine the effect of the diazomethane treatment on stability toward electrochemical cycling. Hydrogen-terminated wafers employed as electrodes for reduction of 1 mM $Ru(NH_3)_6^{3+}$ yielded normal, sharp voltammograms in aqueous solution, but gradual oxidation of the surface resulted in an increase in overpotential (cathodic peak shift to −ve potentials) due to a combination of changes in flatband potential and increased series resistance (Figure 4a,c). This effect is well-known in silicon electrochemistry. The diazomethane treated surfaces, however, were more stable, and steady-state quasi-reversible voltammograms were obtained on cycling under illumination with no significant drop in peak current nor any detectable shift in peak potential (Figure 4b,d). This indicates that the treated surface is resistant to oxidation in neutral aqueous solution. These CVs also show that the electron transfer to the dissolved redox species is not greatly impeded compared to H-terminated silicon surfaces, as expected for a thin polymeric alkyl layer and a fast outer-sphere redox couple such as $Ru(NH_3)_6^{3+/2+}$. Facile electron transfer has also been reported at *n*-alkyl monolayers on silicon.[72] The anodic peak potential is, however, shifted positively, which may reflect the lower oxidation potential of the holes in the diazomethane treated electrodes (negative shift of flatband potential, vide infra) and the presence of a small tunneling barrier. Stable voltammograms were not obtained if the positive potential limit was increased beyond ca. 0.6 V vs AgCl/0.1 M NaCl, presumably because of anodic oxidation of the surface. The foot of such an oxidation wave is in fact just visible at +0.6 V in Figure 4. The oxidation of silicon electrodes in aqueous media has been much studied.[44,46] A plausible interpretation of our results is that the chemical oxidation (O_2, H_2O) of the surface is hindered by diazomethane treatment since the Si−C bond is less reactive than Si−H, but that the electrochemical oxidation is still feasible if the driving force is sufficiently high since the layer is too thin to prevent access of water molecules.

STM images of the *n*-Si(111) surfaces were obtained using bias voltages of ≥+0.7 V and tunneling currents of 0.5 nA (Figure 5). The silicon surfaces were prepared by etching in nitrogen-purged solutions as suggested by Wade and Chidsey.[46] Images under vacuum were stable for periods of at least 1 h; however, on continuous imaging in-air, evidence of the formation of insulating patches (low currents, image instability) was seen after 5−10 min. The freshly etched Si(111) surfaces showed the characteristic terrace and step features.[46,66] Figure 5A shows an image of the Si(111) surface after photolysis in diazomethane; the same general surface features are visible, although higher bias voltages were normally required for stable imaging (2.1 V). In contrast to the hydrogen-terminated silicon samples, these images did not change noticeably during imaging in air. The requirement for higher bias voltages to achieve stable imaging is consistent with the presence of a thin insulating layer on the sample. Although the width of the terraces (typically 50−70 nm) is approximately unchanged by the reaction, there is some evidence for roughening of the step edges,[28] which is likely in this case to be due to etching as a result of trace water originating from the $EtOH/H_2O$ mixture required for preparation of diazomethane. However, the diazomethane treatment appears

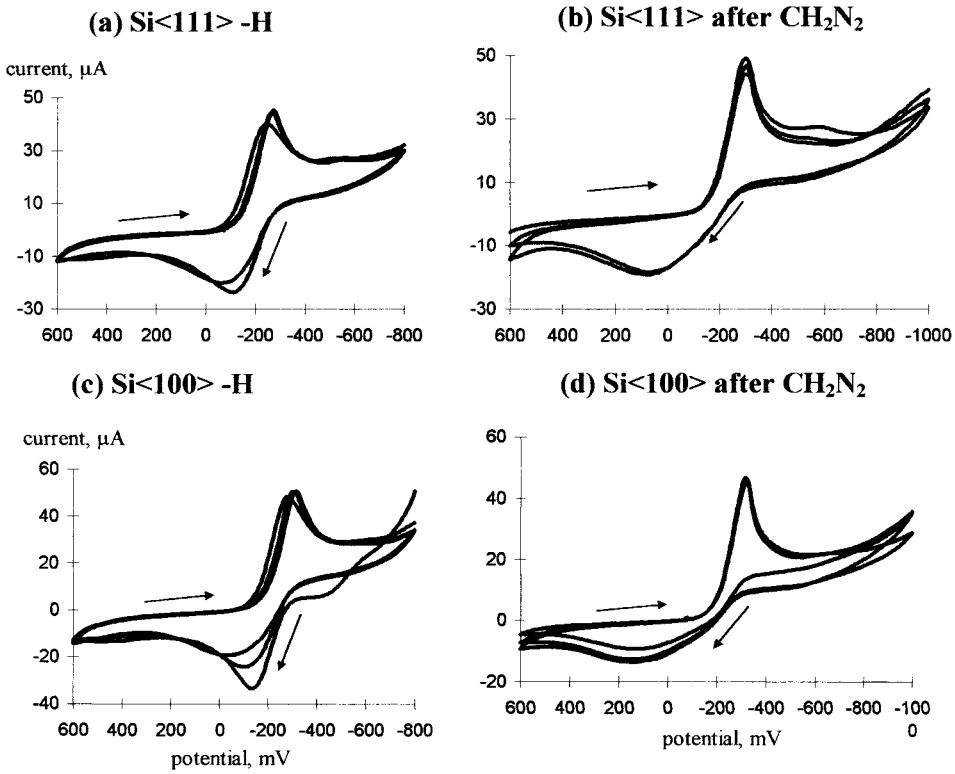

Figure 4. Cyclic voltammograms under illumination by a 100 W tungsten lamp of ⟨100⟩ and ⟨111⟩ oriented, polished *p*-Si wafers in 1 mM $Ru(NH_3)_6^{3+}$ with 0.1 M KCl as electrolyte and a scan rate of 25 mV s^{-1}. (a) HF-etched, ⟨111⟩ oriented, (b) as (a), but after photolysis in ether/diazomethane for 2h, (c) HF-etched, ⟨100⟩ oriented and (d) as (c), but after photolysis in ether/diazomethane for 2h.

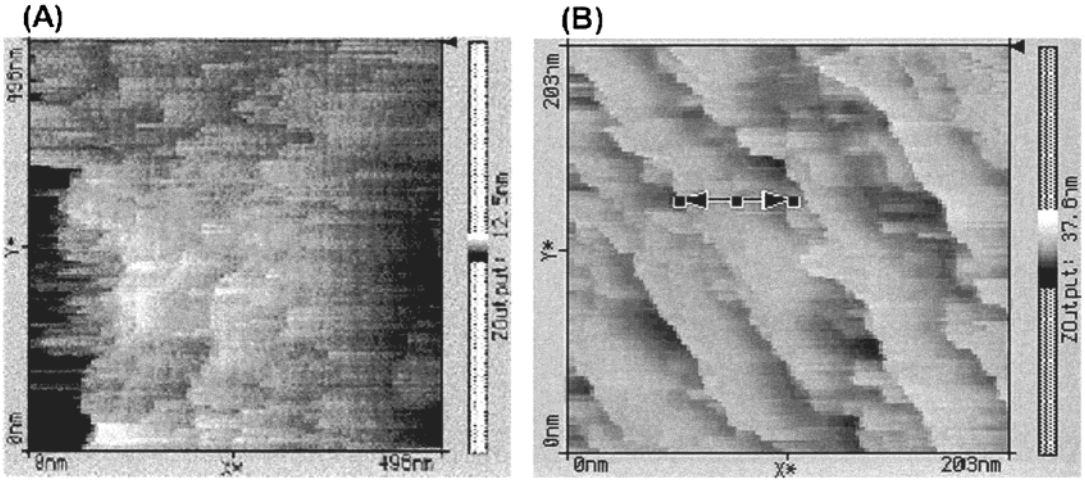

Figure 5. (A) STM image of diazomethane/*hν*-treated *n*-Si(111) in air (phosphorus-doped, $\rho = 1-20\ \Omega$ cm). Tip−sample bias = +2.1 V, tunneling current = 0.5 nA. 0.069 s $line^{-1}$, no filter applied. (B) Hydrogen-terminated *n*-Si(111) in low vacuum (phosphorus-doped, $\rho = 1-20\ \Omega$ cm). Tip−sample bias = +0.72 V, tunneling current = 0.5 nA. 0.069 s $line^{-1}$, no filter applied.

to preserve the essence of the surface structure, and the formation of islands typical of oxide growth[69] was not observed.

Impedance Spectroscopy of p-Si(111) Electrodes. Impedance spectroscopy of diazomethane-treated and hydrogen-terminated p-Si electrodes over the frequency range 200−5000 Hz in aqueous 0.1 M NaCl showed behavior consistent with a series RC combination over a range of potentials and no evidence for faradaic impedances. The flat band potential could be obtained from a nonlinear least-squares fit of the capacitance-potential data. We treated the interfacial capacitance in a manner similar to the analysis of Allongue and co-workers[66,67] as the series combination of the space-charge capacitance in the semiconductor and a constant capacitance due to the monolayer and the aqueous double layer. The space-charge capacitance was obtained from the standard Poisson−Boltzmann treatment,[70] and the contribution of the diffuse layer in the electrolyte was ignored. Reasonable fits were obtained, although there is some evidence for charging of electronic states at the silicon surface in the data around the flatband potential where the fit to theory is less good (Figure 6). The data for n-Si electrodes showed some effects attributable to faradaic processes at negative potentials and was therefore not analyzed. Faradaic currents due to hydrogen evolution have also been reported in the study of Si−C bonded monolayers in H_2SO_4/HF solutions by Allongue and co-workers.[67]

The flatband potential of Si(111)−H electrodes was +0.40 V vs Ag/AgCl in 0.1 M NaCl, and the shift of the flatband potential after photolysis in the presence of diazomethane is

TABLE 2: Computed Dipole Moments and Polarizabilities in the Direction Normal to the Plane of the Three Equivalent Si Atoms Representing the Si(111) Surface[a]

molecule	finite field calculation[b]	dipole moment, atomic units	polarizability, atomic units
$(H_3Si)_3Si-H$	MP4/6-311G(d,p)	0.0429	92.84
$(H_3Si)_3Si-OH$	MP4/6-311G(d,p)	0.0904	95.55
$(H_3Si)_3Si-CH_3$	MP4/6-311G(d,p)	0.3277	111.34
$(H_3Si)_3Si-O-CH_3$	MP4/6-311G(d,p)	0.2291	113.46
Polymer: Figure 3b	RHF/SBK-effective core potential basis set	0.6277	298.42

[a] Positive values correspond to negative charge on Si. MP4 calculations included triple excitations, i.e., MP4SDTQ. All geometries were computed at the MP2/6-311G(d,p) level except for the polymeric species, which was optimized using a density functional method (B3LYP/6-31G(d). [b] Hartree−Fock and MPn computations employed the PC GAMESS version of the GAMESS (US) quantum chemistry package. DFT computations employed the software TITAN.[55]

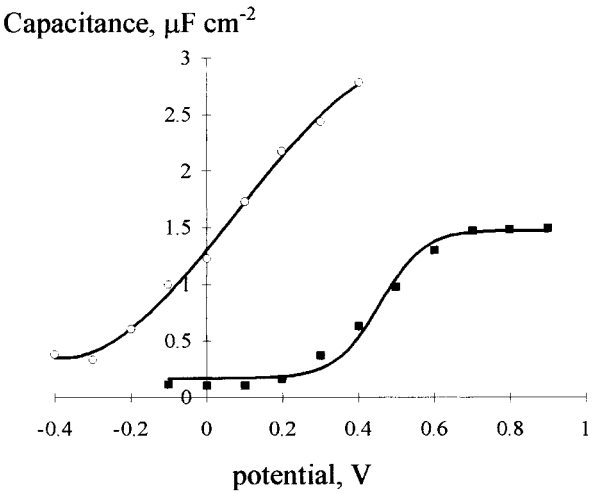

Figure 6. Fitted capacitance-potential curves for diazomethane/$h\nu$-treated (○) and hydrogen-terminated (■) *p*-Si(111) electrodes in 0.1 M NaCl electrolyte.

-0.35 ± 0.04 V with respect to a hydrogen-terminated Si(111) surface (Figure 6). This value is similar to that observed recently for Si−C bonded, short-chain monolayers, e.g., ethyl, prepared by reaction of Grignard reagents with Si(111) surfaces.[67] A comparison of the experimental flatband shifts with the dipole moments calculated for molecules of the form $(H_3Si)_3Si-X$ where X = H, OH, or CH_3 provides a partial, qualitative explanation. The dipole moment normal to the plane containing the three equivalent Si atoms in these molecules is an approximation to the dipole moment normal to the Si(111) surface since the Si−H bonds are relatively nonpolar. Finite field ab initio calculations on such small molecule models (Table 2 and Supporting Information 2) show that the component of the permanent dipole moment normal to the Si(111) surface is very small for Si(111)−H (∼0.04 atomic units) but is quite significant for Si(111)−CH_3 and other short alkyl chains (0.3−0.4 atomic units). Similar dipole moments per unit area are also found for the polymeric species of Figure 3b. The sign of the dipole moment is such that the flatband potential would be expected to shift in a negative direction on alkylation, as observed. Measurement of the apparent tunneling barrier height at Si(100) by an STM technique has also shown that a monolayer of cyclopentene molecules bound via Si−C had a dipole moment oriented toward the surface (δ^+ on molecule, δ^- on surface) with a magnitude of 0.146 atomic units.[71] An examination of the Mulliken and Löwdin atomic charges for $(H_3Si)_3Si-CH_3$ at the MP2/6-31G(d,p) level shows that the Si atom bonded to the methyl group carries only a small positive charge (Mulliken: 0.054, Löwdin: 0.088 atomic units), whereas the carbon atoms carry significant negative charges (−0.53, −0.47 atomic units) and the hydrogen atoms on the alkyl chain are δ^+. In the case of longer alkyl chains, e.g., $(H_3Si)_3Si-C_6H_{13}$, a similar pattern of charges is observed with values −0.38/−0.33 atomic units on the C atom bonded to Si and slightly smaller charges on the other carbon atoms. Within the limitations of the atomic-charge analysis, the Si−C bond is essentially nonpolar, as expected on the basis of electronegativities, but the C−H bonds are slightly polar, and this results in a significant overall dipole moment. A precise calculation of the flatband potential shift upon diazomethane treatment cannot be made without more detailed structural information on the monolayer; however, the sign and magnitude of the experimental value are consistent with a polymeric hydrocarbon layer on the silicon surface.

Conclusions

Photolysis of ethereal solutions of diazomethane using the $\lambda = 365$ nm mercury line in the presence of hydrogen-terminated porous or single-crystal silicon results in the formation of Si−C bonded alkyl groups on the surface. The FTIR spectra are consistent with a polymeric species in which the major IR bands are due to $-CH_2-$ groups. The reaction occurs on both porous and polished single crystal wafers, and the first step is most likely direct insertion of methylene into the Si−H bonds. Porous silicon surfaces were found to undergo significant oxidation in parallel to alkylation; however, the oxide could be removed by washing with aqueous HF without affecting the integrated intensity of the bands due to alkyl species. Single-crystal wafers that had been reacted with diazomethane by this process were found to display stable cyclic voltammetric behavior in aqueous solutions of $Ru(NH_3)_6^{3+}$ with no shift in cathodic peak potential, in contrast to the behavior of hydrogen-terminated silicon. STM images of these surfaces showed terrace and step features essentially unchanged compared to the underlying silicon substrate. The measured flatband potentials of the diazomethane-treated surfaces are shifted in a negative direction (−0.35 V) with respect to hydrogen-terminated silicon electrodes as previously observed for Si(111) modified with short chain alkanes.[67] The CV, impedance, STM, and FTIR data are consistent with a thin polymeric layer, which confers significant protection against oxidation but does not block electron transfer.

Acknowledgment. We acknowledge EPSRC for funding under grants GR/M69104 and AF/990206. We also acknowledge an anonymous referee for important suggestions concerning the infrared data.

Supporting Information Available: (1) Optical micrographs (×500 magnification) of porous silicon prepared at high and low current density. (2) More detailed table of results of the finite field calculations at various levels of theory. This material is available free of charge via the Internet at http://pubs.acs.org.

References and Notes

(1) Sailor, M. J.; Lee, E. J. *Adv. Mater*. **1997**, *9*, 783−793 and references therein.

(2) Sailor, M. J.; Heinrich, J. L.; Lauerhaas, J. M. *Stud. Surf. Sci. Catal.* **1997**, *103*, 209.

(3) Buriak, J. M. *Chem. Commun.* **1999**, 1051 and references therein.

(4) Waltenburg, H. N.; Yates, J. T. *Chem. Rev.* **1995**, *95*, 1589.

(5) Bansal, A.; Li, X.; Lauermann, I.; Lewis, N. S.; Weinberg, W. H. *J. Am. Chem. Soc.* **1996**, *118*, 7225−7226.

(6) Bansal, A.; Lewis, N. S. *J. Phys. Chem. B* **1998**, *102*, 1067. Bansal, A.; Lewis, N. S. *J. Phys. Chem. B* **1998**, *102*, 4058.

(7) Royea, W. J.; Juang, A.; Lewis, N. S. *Appl. Phys. Lett.* **2000**, *77*, 1988.

(8) Bondarenko, V. P.; Yakovtseva, V. A. In *Properties of Porous Silicon*; Canham, L. T., Ed.; INSPEC: London, 1997; p 343. Sailor, M. J. In *Properties of Porous Silicon*; Canham, L. T., Ed.; INSPEC: London, 1997; p 364.

(9) Sieval, A. B.; Demirel, A. L.; Nissink, J. W. M.; Linford, M. R.; van der Maas, J. H.; de Jeu, W. H.; Zuilhof, H.; Sudholter, E. J. R. *Langmuir* **1998**, *14*, 1759.

(10) Vuillaume, D.; Boulas, C.; Collet, J. *Appl. Phys. Lett.* **1996**, *69*, 9.

(11) Letant, S. E.; Sailor, M. J. *Adv. Mater*. **2001**, *13*, 335.

(12) Weldon, M.; Stefanov, B. B.; Raghavachari, K.; Chabal, Y. J. *Phys. Rev. Lett.* **1997**, *79*, 2851.

(13) Strother, T.; Hamers, R. J.; Smith, L. M. *Nucleic Acids Res*. **2000**, *28*, 3535.

(14) Sieval, A. B.; Linke R.; Zuilhof, H.; Sudholter, E. J. *R. Adv. Mater.* **2000**, *12*, 1457.

(15) Wagner, P.; Nock, S.; Supdich, J. A.; Volkmuth, W. D.; Chu, S.; Cicero, R. L.; Wade, C. P.; Linford, M. R.; Chidsey, C. E. D. *J. Struct. Biol.* **1997**, *119*, 189.

(16) Jeon, N. L.; Choi, I. S.; Whitesides, G. M.; Kim, N. Y.; Laibinis, P. E.; Harada, Y.; Finnie, K. R.; Girolami, G. S.; Nuzzo, R. G. *Appl. Phys. Lett.* **1999**, *75*, 4201.

(17) Juang, A.; Scherman, O. A.; Grubbs, R. H.; Lewis, N. S. *Langmuir* **2001**, *17*, 1321.

(18) Stewart, M. P.; Buriak, J. M. *Angew. Chem., Int. Ed. Engl.* **1998**, *37*, 3257.

(19) Buriak, J. M.; Allen, M. J. *J. Am. Chem. Soc.* **1998**, *120*, 1339.

(20) Choi, H. C.; Buriak, J. M. *Chem. Mater.* **2000**, *12*, 2151.

(21) Ulman, A. *An Introduction to Ultrathin Organic Films: From Langmuir−Blodgett to Self-assembly*; Harcourt Brace Jovanovic: Boston, 1991 and references therein.

(22) (a) Linford, M. R.; Chidsey, C. E. D. *J. Am. Chem. Soc*. **1993**, *115*, 12631−12632. (b) Linford, M. R.; Fenter, P.; Eisenberger, P. M.; Chidsey, C. E. D. *J. Am. Chem. Soc*. **1995**, *117*, 3145−3155.

(23) Chazalviel, J.-N. *J. Electroanal. Chem*. **1987**, *233*, 37.

(24) Kim, N. Y.; Laibinis, P. E. *J. Am. Chem. Soc.* **1997**, *119*, 2297−2298.

(25) Cleland, G. C.; Horrocks, B. R.; Houlton, A. *J. Chem. Soc., Faraday Trans.* **1995**, *91*, 4001.

(26) Haber, J. A.; Lauermann, I.; Michalak, D.; Vaid, T. P.; Lewis, N. S. *J. Phys. Chem. B* **2000**, *104*, 9947.

(27) Eagling, R. D.; Bateman, J. E.; Goodwin, N. J.; Henderson, W.; Horrocks, B. R.; Houlton, A. *J. Chem. Soc., Dalton Trans*. **1998**, 1273.

(28) Boukherroub, R.; Morin, S.; Sharpe, P.; Wayner, D. D. M. *Langmuir* **2000**, *16*, 7429.

(29) Zhu, X. Y.; Mulder, J. A.; Bergerson, W. F. *Langmuir* **1999**, *15*, 8147.

(30) Sung, M. M.; Kluth, G. J.; Yauw, O. W.; Maboudian, R. *Langmuir* **1997**, *13*, 6164−6168.

(31) Hovis, J. S.; Hamers, R. J. *J. Phys. Chem. B* **1998**, *102*, 9581.

(32) Boukherroub, R.; Wayner, D. D. M. *J. Am. Chem. Soc.* **1999**, *121*, 11513.

(33) Sieval, A. B.; Vleeming, V.; Zuilhof, H.; Sudholter, E. J. R. *Langmuir* **1999**, *15*, 8288.

(34) Cicero, R. L.; Linford, M. R. Chidsey, C. E. D. *Langmuir* **2000**, *16*, 5688.

(35) Effenberger, F.; Gotz, G.; Bidlingmaier, B.; Wezstein, M. *Angew. Chem., Int. Ed. Engl.* **1998**, *37*, 2462.

(36) de Villeneuve, C. H.; Pinson, J.; Bernard, M. C.; Allongue, P. M. *J. Phys. Chem. B* **1997**, *101*, 2415.

(37) Zazzera, L. A.; Evans, J. F.; Deruelle, M.; Tirrell, M.; Kessel, C. R.; McKeown, P. *J. Electrochem. Soc*. **1997**, *144*, 2184−2189.

(38) Warntjes, M.; Vieillard, C.; Ozanam, F.; Chazalviel, J.-N. *J. Electrochem. Soc.* **1995**, *142*, 4138.

(39) Bateman, J. E.; Horrocks, B. R.; Houlton, A. *J. Chem. Soc., Faraday Trans.* **1997**, *93*, 2427.

(40) Boukherroub, R.; Morin, S.; Bensebaa, F.; Wayner, D. D. *Langmuir* **1999**, *15*, 3831.

(41) (a) Ozanam, F.; Vieillard, C.; Warntjes, M.; Dubois, T.; Pauly, M.; Chazalviel, J.-N. *Can. J. Chem. Eng.* **1998**, *76*, 1020. (b) Dubois, T.; Ozanam, E.; Chazalviel, J.-N. *Proc. Electrochem. Soc.* **1997**, *97-7*, 296.

(42) Gurtner, C.; Wun, A. W.; Sailor, M. J. *Angew. Chem., Intl. Ed. Engl*. **1999**, *38*, 1966.

(43) Fidelis, A.; Ozanam, F.; Chazalviel, J.-N. *Surf. Sci. Lett.* **2000**, *L7*, 444.

(44) Allongue, P. M.; Costa-Kieling, V.; Gerischer, H. *J. Electrochem. Soc.* **1993**, *140*, 1018.

(45) Song, J. H.; Sailor, M. J. *Inorg. Chem.* **1998**, *37*, 3355.

(46) Wade, C. P.; Chidsey, C. E. D. *Appl. Phys. Lett.* **1997**, *71*, 1679.

(47) Kramer, K. A. W.; Wright, A. N. J. *Chem. Soc.* **1963**, 3604.

(48) Simons, J. W.; Mazac, C. J. *Can. J. Chem.* **1967**, *45*, 1717.

(49) Mazac, C. J.; Simons, J. W. *J. Am. Chem. Soc*. **1968**, *90*, 2484.

(50) Kirmse, W. Carbene Chemistry in *Organic Chemistry*, 2nd ed.; Blomquist, A. T., Wasserman, H., Eds.; Academic Press: New York, 1971; Vol. 1, Ch. 7, pp 209−223 and Ch. 11, pp 407−409.

(51) Sommer, L. H.; Ulland, L. A.; Ritter, A. *J. Am. Chem. Soc*. **1968**, *90*, 4486.

(52) Kirmse, W. Carbene Chemistry in *Organic Chemistry*, 1st ed.; Blomquist, A. T., Wasserman, H., Eds.; Academic Press: New York, 1964; Vol. 1, Ch. 2, pp 8−18.

(53) A 43 g (0.2 mol) portion of *N*-methyl-*N*-nitrosotoluene-*p*-sulfonamide was dissolved in 250 mL ether and added dropwise over 45 min to a solution of 10 g KOH in 50 mL 96% ethanol/15 mL H_2O. The diazomethane was distilled from a water bath under a stream of dry nitrogen and collected in 500 mL ether in a receiving flask that was cooled on ice. The final ethereal solution contains ca. 70% yield of diazomethane. **CARE: explosion risk avoid ground glass joints and sharp edges**.

(54) Bateman, J. E.; Eagling, R. D.; Houlton, A.; Horrocks, B. R. *J. Phys. Chem. B* **2000**, *104*, 5557−5565.

(55) TITAN is a combination of Jaguar 3.5, Schrodinger Inc., 1500 S.W. First Avenue, Suite 1180 Portland, OR 97201 and Spartan, Wavefunction Inc. 18401 Von Karman Ave., Ste. 370, Irvine, CA 92612.

(56) Granovsky, A. A. www http://classic.chem.msu.su/gran/gamess/index.html.

(57) Schmidt, M. W.; Baldridge, K. K.; Boatz, J. A.; Elbert, S. T.; Gordon, M. S.; Jensen, J. J.; Koseki, S.; Matsunaga, N.; Nguyen, K. A.; Su, S.; Windus, T. L.; Dupuis, M.; Montgomery, J. A. *J. Comput. Chem.* **1993**, *14*, 1347−1363.

(58) Bateman, J. E.; Eagling, R. D.; Worrall, D. R.; Horrocks, B. R.; Houlton, A. *Angew. Chem., Intl. Ed. Engl.* **1998**, *37*, 2683.

(59) Ogawa, H.; Ishikawa, K.; Inomata, C.; Fujimura, S. *J. Appl. Phys.* **1996**, *79*, 472.

(60) Takahagi, T.; Ishitani, A.; Kuroda, H.; Nagasawa, Y.; Ito, H.; Wakao, S. *J. Appl. Phys.* **1990**, *68*, 2187.

(61) Ogawa, H.; Hattori, T. *Appl. Phys. Lett.* **1992**, *61*, 577.

(62) Bateman, J. E.; Eagling, R. D.; Horrocks, B. R.; Houlton, A.; Worrall, D. R. *Chem. Commun*. **1997**, 2275−2276.

(63) Amato, G.; Boarino, L.; Brunetto, N.; Rossi, A. M.; Steni, R.; Bellone, A.; Schirone, L.; Sotgiu, G. *Solid State Phenom.* **1997**, *54*, 50.

(64) Theiss, W.; Hilbrich, S.; Arens-Fischer, R.; Berger, M. G.; Mönder, H. *Optical and structural properties of porous silicon nanostructures*; Amato, G., Delerue, C., von Bardeleben, H. J., Eds.; Gordon & Breach: Langhorn, PA, 1996.

(65) Allongue, P.; de Villeneuve, C. H.; Pinson, J.; Ozanam, F.; Chazalviel, J.-N.; Wallart, X. *Electrochim. Acta* **1998**, *43*, 2791.

(66) Allongue, P.; de Villeneuve, C. H.; Pinson, J. *Electrochim. Acta* **2000**, *45*, 3241.

(67) Yu, H. Z.; Morin, S.; Wayner, D. D. M.; Allongue, P.; de Villeneuve, C. H. *J. Phys. Chem. B* **2000**, *104*, 11157.

(68) Sieval, A. B.; van den Hout, B.; Zuilhof, H.; Sudholter, E. J. R. *Langmuir* **2000**, *16*, 2987.

(69) Neuwald, U.; Hessel, H. E.; Feltz, A.; Memmert, U.; Behm, R. J. *Appl. Phys. Lett.* **1992**, *60*, 1307.

(70) Dewald, J. F. *J. Phys. Chem. Solids* **1960**, *14*, 155.

(71) Akiyama, R.; Matsumoto, T.; Kawai, T. *Phys. Rev. B* **2000**, *62*, 2034.

(72) Yu, H. Z.; Boukherroub, R.; Morin, S.; Wayner, D. D. M. *Electrochem. Commun.* **2000**, *2*, 562.

(73) Socrates, G. *Infrared characteristic group frequencies: tables and charts*, 2nd ed.; Wiley: Chichester, New York, 1994; Ch. 18.